SPIE Vol 2384, p. 101-108, 1995.

# Time-resolved contrast in near-field scanning optical microscopy of semiconductors

A.H. La Rosa, C.L. Jahncke, and H.D. Hallen,

Physics Department, North Carolina State University,
Raleigh, North Carolina 27695-8202

## ABSTRACT

We demonstrate the ability of near-field scanning optical microscopy (NSOM) technique to detect inhomogeneities of the dynamics of excess carriers in oxidized silicon wafers. NSOM is used to improve the spatial resolution of a standard IR-scattering optical technique, which is carried out in a non contact fashion. Continuous wave infrared light is used as a detector of the time dependent carrier population produced by a pulsed visible laser. We will show high resolution images of carrier lifetime, and discuss some aspects of the NSOM measurement that differentiate it from its far field counterpart.

**Keywords:** near-field optics, time resolved, carrier lifetime, carrier dynamics, silicon

## 1. BACKGROUND

In the current trend of electronic device miniaturization reaching the nanometric scale[1], non-contact characterization techniques offering high spatial resolution are becoming essential. Especially desirable are those which can measure the defect properties, as defects can have dramatic effects on small device performance. Also important is the physics underlying carrier dynamics within nanostructures, if indeed sub micron devices are to be put into large scale production[2]. In this paper we describe our efforts at lifetime measurement of excess carriers in silicon samples. The work was performed with the implementation of near-field scanning optical microscopy (NSOM).

Carrier lifetime ($\tau$) is heuristically defined as the average time excess carriers exist within a sample before they recombine and are annihilated. During that time they are available to contribute to the conductivity of a sample or they may be collected in a device such as a photodetector. The carrier lifetime is one of the most important parameters used to characterize the quality of semiconductors. A high value of $\tau$ usually indicates a low concentration of impurities and defects which act as trap or recombination centers for carriers. Measurements of $\tau$ with techniques involving conventional optics[3] (referred to here as far-field optics) have received preference due to their non-invasive nature. However, when very fine lateral resolution is required, far-field optics encounters a limitation: features smaller than $\lambda/2$ can not be resolved[4]. Here $\lambda$ is the wavelength of the radiation being used. Typically wavelengths of 0.5 $\mu$m for green light and 1-10 $\mu$m for infrared light are used in these optical lifetime studies. NSOM can alleviate the resolution limitation while maintaining the advantages of an optical measurement. In fact, the resolution of NSOM is sufficiently high that we have to reconsider the definition of what we mean by a local carrier lifetime. This will be discussed in detail below.

The NSOM[5] technique can achieve this high resolution by geometrically constraining the light within a small aperture which is placed in close proximity to the sample. Resolution is determined by the physical size of the aperture and the distance of that aperture from the sample surface, not by the wavelength of the light employed. (The signal intensity, however, is dependent upon the light wavelength for a given configuration, due to the variation in cutoff diameter with wavelength.) The aperture is fabricated by coating the end of a sharpened optical fiber with Al. The sample distance is readily controlled by oscillating this probe and using lateral force feedback[6]. Resolution of ~ 20 nm has already been achieved[5]. Two recent examples of the power of NSOM are the following. First[7], measurements of fluorescence lifetime of single molecules dispersed on glass or silica surfaces have been made by looking at the fluorescent decay while at a stationary point. Second, high lateral resolution combined with photoluminescence spectroscopy at low temperature has revealed the localized nature of individual optically active emitters in quantum well heterostructures; thus paving the way to study their corresponding dynamics[8]. We present here an alternative development of NSOM: its implementation as an *imaging* tool to study the dynamics of excess carriers in semiconductor devices. We concentrate on obtaining images for which the contrast mechanism is a time-dependent property of the sample, and attempt to relate them to important sample characteristics.

Specifically, visible laser light is modulated to create a time-varying excess carrier distribution. This distribution is monitored by noting its effect on continuous wave infrared (IR) laser radiation also illuminating the sample. In the experiment reported here, both types of light are input through the same NSOM probe aperture. This configuration insures high lateral resolution, and avoids mismatch in the sample regions illuminated by either laser light. Although heat effects on the tip are caused by the visible light, they produce only a background whose influence in our signal can be minimized by working at a proper modulation frequency. The sample used in these studies was oxidized silicon. The dominant source of the contrast observed in our images comes from the time-dependent number of carriers available to scatter IR radiation. We are directing our efforts to measure the change in the transmitted signal, $\Delta\phi_T$, in real time, but for now we find it more convenient for imaging purposes to detect the signal synchronously with a lock-in amplifier. This reduces the computational load during acquisition and improves the signal to noise ratio.

In section 2 we describe the drastic improvements we have made to the infrared detection system since our previous work[9]. Section 3 outlines the generation and recombination process of excess carriers. We show that a rough signal estimation agrees with the measured modification of the transmitted infrared radiation. Section 4 includes the time-resolved NSOM image of an oxidized silicon wafer obtained under the modality described above. We include the corresponding topographic and IR transmission images, also taken under the NSOM modality, and highlight their differences. Tip heating and its influence on our measurements are also discussed. Section 5 compares our technique to the more conventional far-field measurements, and points out some of the qualitatively different features NSOM engenders.

## 2. EXPERIMENTAL TECHNIQUE

The apparatus has been described previously[9]. In the methodology we follow (see figure 1), visible laser light is modulated by an acousto optic modulator. The corresponding variation in the

IR (1.15 $\mu$m) transmission intensity caused by the electron-hole (e-h) pairs is detected and fed into a lock-in amplifier for synchronous detection which generates our signal. Note that the sample absorbs all of the visible light so that it acts as a filter which passes only the IR signal to the detector. Not shown in the figure is the implementation of sample-probe distance regulation. This is accomplished in a standard fashion [6,10] using illumination of the fiber tip from the side and detection of the nearly-forward scattered light.

The noise floor of the IR detection system has been drastically reduced. Several improvements include a) a new two stage pre amplifier[11]. The advantage of a two stage system is that it gives us the ability to optimize the combination of signal to noise and bandwidth required for this work. The first stage has a gain of $10^8$. The second stage is a bandwidth broadener that provides 100 kHz bandwidth. The spectral noise density at moderate frequencies is limited by the Johnson current noise of the gain resistor combined with the shunt resistance of the diode detector, ~30 fA/(Hz)$^{1/2}$ at 10 kHz. This is increased by 1/f noise at low frequencies, by about a factor of 3 near 200 Hz, and by the bandwidth broadener at high frequencies, to 100 fA/(Hz)$^{1/2}$ at 100 kHz. Since the noise background is better than $10^{-4}$ nW/ Hz$^{1/2}$ , detection of nanowatt power levels from a NSOM probe is not a problem. Also, depending on the light output power from the probe (which is governed by the aperture size), this value sets the contrast level we can currently detect. For a 100 nW output and ~ 2 Hz detector bandwidth, a mechanism that modifies the infrared signal to one part in $10^6$ would provide a signal close to the noise limit. b) The preamplifier assembly has been constructed around and adjacent to the infrared diode assembly, in order to reduce the input capacitance of the preamplifier. This further minimizes the possibility of unwanted oscillations in the electrical signal and aids in the bandwidth optimization. c) The photo diode is now InGaAs, from EPITAXX (ETX 500T), which provides low noise performance at room temperature. This reduces thermal gradients within the microscope vicinity, which can affect reproducibility in our scanning system by inducing thermal drift in the microscope. Due to these improvements, the major source of noise in the measurement process is no longer the detection of the IR light. Rather, the noise is limited by the stability of the IR laser source. We are currently working on reducing those levels to further improve the system signal to noise level.

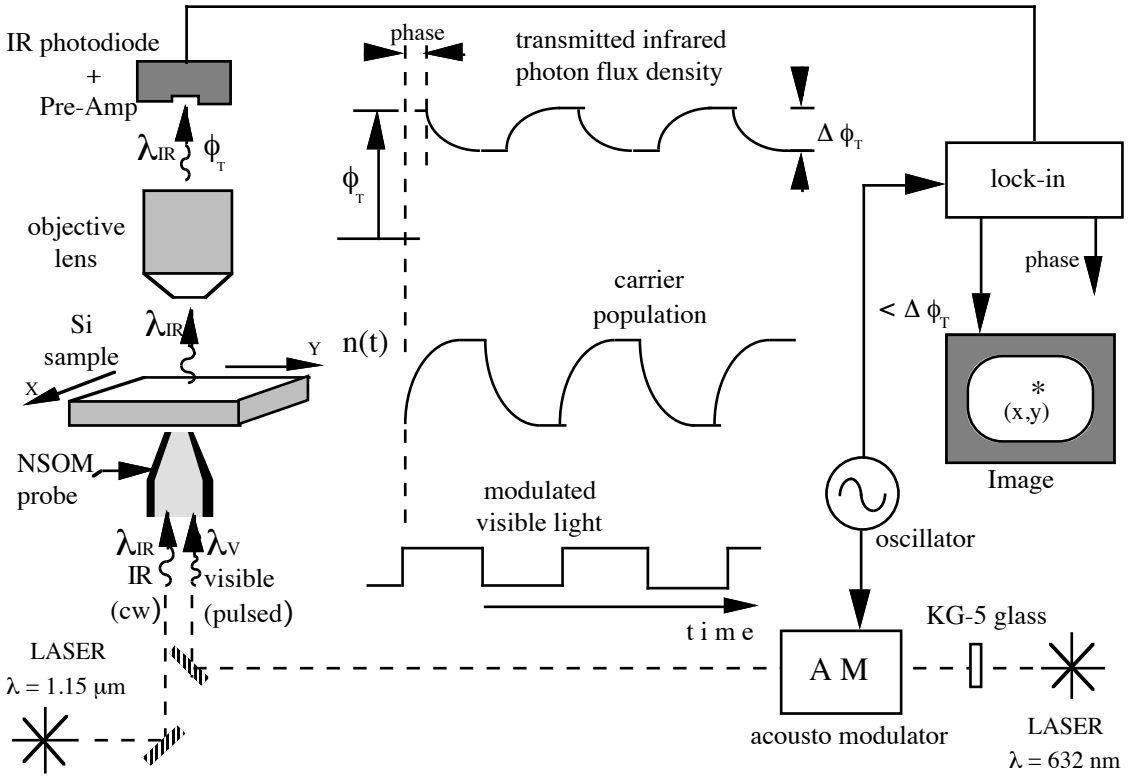


Fig. 1 Schematic of the process to extract information of the local dynamics of excess carriers in a semiconductor. Left side : optical path of the IR radiation. Center: A timing diagram of the process. Right : Synchronous detection of the transmitted infrared signal. An image is constructed by repeating this process as the probe is scanned across the sample.

The visible (pumping) light is produced by a He-Ne laser ($\lambda = 632$ nm). Care is taken to filter any IR component of this He-Ne laser by using a 2 mm thick KG5 glass[12] in front of the output window. This reduces the IR component by a factor of $5 \times 10^4$. The probe IR light ($\lambda = 1.15$ μm) is also produced by a He-Ne laser. Both lasers are coupled into a fiber optic Y. The other end of the Y is coupled to the tapered fiber probe of the NSOM.

The sample used in this experiment is an oxidized, phosphorus doped n-type silicon wafer. The silicon dioxide film grown on the wafer is 60-70 nm in thickness. The dopant level is about $4 \times 10^{14}$ atoms/cm$^3$ corresponding to a 10 ohm-cm resistivity. The surface recombination velocity of the oxidized n-type wafer has been estimated to be on the order of 10 cm/sec. The minority carrier effective lifetime of this sample, $\tau_p = 1.6$ ms, was measured at room temperature using a laser/microwave method[13] (LIFETECH-88, SEMITEX Co., Ltd). This value should be considered as an average lifetime value for a macroscopic sample size.

## 3. GENERATION AND DIFFUSION OF CARRIERS

In this section we will discuss the generation and diffusion of carriers. Employing a simple theoretical model, we will perform an order of magnitude calculation of the carrier density, $\delta p$, and the detected signal, $\Delta\phi_T/\phi_T$, where $\phi_T$ is the transmitted signal. We will briefly mention the effects of refractive index changes.

First, let us estimate the volume of the generation region. Since the probe is placed close to the surface, the lateral size of the illuminated area is approximately the same as the aperture size for which we will use 200 nm. The depth that the light will penetrate into the sample is determined by the absorption coefficient which is $\sim 3\text{x}10^3$ cm$^{-1}$ for red light. Qualitatively, then, we have a wavefront of radiation that penetrates the sample to a depth of $\Delta z \sim 3.5$ $\mu$m. The optical field spreads as it enters the sample, but the high index of silicon limits most of the optical beam to a narrow one. We will take the volume of interaction, where the e-h pairs are created, to be $\Delta V = 1.0 \times 10^{-13}$ cm$^3$.

Next, we estimate the generation rate of e-h pairs. For 1 mW of visible red light injected into the fiber at the far end from the probe, a rate of $J_{in} = 3.2 \times 10^{15}$ photons/sec is obtained. Assuming a probe throughput efficiency of $g = 10^{-2}$, and a reflection coefficient from the silicon surface of $R = 0.3$, the rate of photons entering the excitation region is $J_o = 2.2 \times 10^{13}$ photons/s. If each photon generates one e-h pair, the average generation rate we obtain is $G = J_o/\Delta V$. The generation of e-h pairs is balanced by diffusion and the recombination process as the system tends towards a steady state while the visible light is on. What is relevant in our experiment is the magnitude of the carrier concentration along the path sensed by the IR radiation, which coincides with the excitation region. To that effect, let us consider the equation governing the steady state:

$$D\nabla^2(\delta p) - (\delta p)/\tau + G = \partial(\delta p)/\partial t = 0 \qquad (1)$$

Here $\delta p = \delta n$, $D = 2D_eD_p/(D_e+D_p)$ is the ambipolar diffusion coefficient (at $10^{17}$ - $10^{18}$ cm$^{-3}$ impurity concentration $D \sim 10$ cm$^2$/s), $\tau = 1.6$ ms is the carrier lifetime.

For our estimates, we will not solve the problem for our complicated geometry but will use a spherically symmetric solution in which the generation region is a small hemisphere with volume $\Delta V$ and radius $r_a$. The solution at the origin is

$$\delta p(0) = 2J_o/(D\Delta V)\, r_a^2/2 = 3.8 \times 10^{16} \text{ holes/cm}^3 \qquad (2)$$

for small $r_a/(D\tau)^{1/2}$ . The factor of 2 results since the carriers are constrained to a half-plane. The effective carrier density, n, will be twice this since $\delta p = \delta n$. Therefore, $n = 10^{17}$ carriers/cm$^3$.

With high enough concentration levels a variety of physical phenomena can lead to a measurable modification of the IR transmission signal. In the free carrier absorption phenomena[14,15], carriers in their respective band can undergo transitions in the same band by

absorbing IR radiation. The absorption coefficient of carriers is given by $\alpha_{fc}$ = ($3.7 \times 10^{-18}$ $cm^2/\mu m^2$) $\lambda^2$ n, where $\lambda$ is the IR wavelength (1.15 $\mu$m in our case). For the number of carriers, we use the calculation above. The corresponding absorption coefficient due to the presence of excess carriers is $\alpha_{fc} = 0.54\ cm^{-1}$. The corresponding relative change in the transmission signal is given by

$$(\Delta\phi_T)/\phi_T = -\alpha_{fc}\,\Delta z. \qquad (3)$$

For $\Delta z = 3.5\ \mu m$ we obtain $(\Delta\phi_T)/\phi_T = -1 \times 10^{-4}$.

Another mechanism for generating $(\Delta\phi_T)/\phi_T$ originates in the change of the reflection coefficient caused by the presence of excess carriers. The relative change of the reflection coefficient is given by $\Delta R/R \sim 0.5 \times (\omega_p/\omega_{IR})^2$, where $\omega_p$ is the population dependent plasma frequency, and $\omega_{IR}$ is the angular frequency of the incident IR radiation[16]. Note that since $\omega_p \propto \sqrt{n}$, $\Delta R/R$ depends linearly on the carrier density n. In our case $\omega_{IR} = 1.64 \times 10^{15}$ /s and the plasma frequency corresponding to $n = 10^{17}\ cm^{-3}$ is $\omega_p \sim 3 \times 10^{12}\ s^{-1}$, giving $\Delta R/R \sim 1.6 \times 10^{-6}$, which is smaller than that from the free carrier absorption process.

Currently the experimental signal,$(\Delta\phi_T)/\phi_T$, that we are observing is on the order of $10^{-4}$. What we have shown in this order of magnitude calculation is that the visible radiation from the probe is sufficient to produce a population of e-h pairs which is detectable with the IR scattering technique. Certainly the value $(\Delta\phi_T)/\phi_T$ will be influenced by the particular environment surrounding the tested location. The above calculation assumes that the sample is everywhere uniform. Such a sample would not require the use of NSOM. However, these calculations represent a starting point from which to obtain a more accurate model of the situation. For example, a nearby defect acting as a recombination center can be modeled as a sink in the diffusion equation, and will effect the carrier density in a region surrounding the defect. A trapping center defect can give rise to a different result.

## 4. EXPERIMENTAL RESULTS

Figure 2 shows four images from the same 7.5x7.5 $\mu m^2$ region of the silicon sample. The upper left shows the topography of the region. Except for some isolated dust particles, we have an essentially flat area (the RMS noise of the shear force feedback signal was ~1 nm). The stability of the instrument was verified by repeating the scan from time to time during the 12 hour experimental session.

The image on the upper right side is the conventional NSOM transmission infrared image, which we take as a diagnostic to insure that no artifacts are present in the time-contrast image. The range of the IR signal across the region is 46 nW. We obtain IR signal at all parts of the image with the average IR signal ~ 100nW.

The time-resolved image relating to free carrier absorption is shown at the bottom left. The signal imaged is the average variation in the IR signal with the visible light on or off, $< \Delta\phi_T >$, and

the observed range is 0.05 nW. The lighter regions correspond to faster recombination time. Right after this image is recorded, we proceed to determine if the visible light is playing its expected role: another image is recorded with the only difference being that the red light was blocked. This is shown at the bottom right of the figure. No contrast is observed.

During the course of our experiment, we have also noticed a small background contribution to the signal originating at the tip itself. Since both IR and visible light are sent through the same aperture, a heating effect caused by the visible pumping laser may cyclically heat the probe tip. This can result in a change in the physical size of the tip through thermal expansion or the optical size of the tip through a variety of mechanisms[17]. Changes in the IR throughput of the probe then

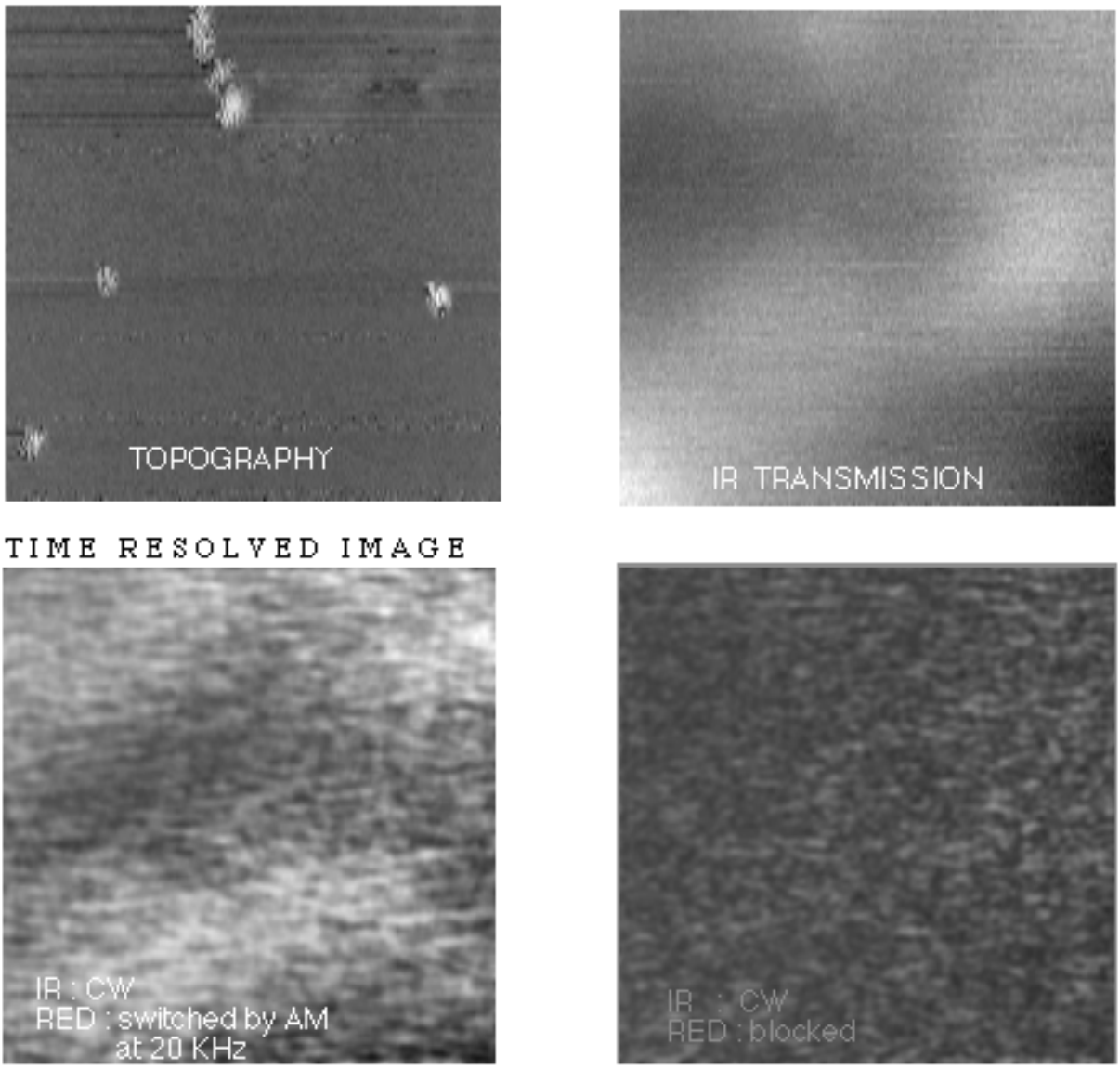


Figure 2 NSOM images from the same region. The time-contrast image is labeled in the lower left, and the image in the lower right is taken under identical conditions except the red light is blocked. It illustrates the system noise level. These four images are raw data, except for the application of plane subtraction.

occurs. This signal does not change as the tip is rastered across the sample and therefore appears as a background signal. It also can be minimized by choosing an appropriate operating frequency. It is instructive to verify that this cyclic heating of the probe tip does not result in a cyclic heating of the local sample region and therefore produce a signal at the operating frequency unrelated to the carrier dynamics. Estimations of the magnitude of the temperature change for nW level power inputs have also been performed in studies of surface modification by STM. It is generally found that the temperature changes are much less than 1 degree, so any effect would be far smaller than that produced by the free carriers.

## 5. DIFFERENCES FROM FAR-FIELD MEASUREMENTS

We have shown that carrier dynamics can be imaged by a non-contact optical method with unprecedented spatial resolution. What we will concentrate upon in this section are several qualitative considerations which should be a part of any heuristic explanation of the process. The first consideration relates to the excitation of carriers, and remains true for any type of NSOM measurement. The second relates to the interpretation of a local lifetime, and results directly from the resolution.

The proximity of the NSOM probe to the surface results in the ability of NSOM to inject light into modes within the sample which would normally be evanescent in a far-field experiment. Specifically, as mentioned above, light with large values of k parallel to the surface can be injected. Although the intensity of such light is not that great, it still provides an opportunity to excite carriers with transitions which would normally not be allowed by momentum selection rules. This may be a useful tool in, for example, studying the quality of epitaxial layers by excitation with a tunable laser source.

At the beginning of the paper, we stated a heuristic meaning for the lifetime constant for the recombination of excess carriers -- the exponential time constant of the change in IR intensity observed. This makes sense for typical measurements which average over large areas of the sample. It is questionable for our measurements since carriers can, if the time constant is long enough, diffuse relatively large distances before recombining. Then carriers which locally interact with the IR light directly beneath the probe tip have, on average, sensed a region of the sample which is large compared to the resolution. Thus, the local measurement contains information from a weighted average of a region of the sample large compared to the local region. This weighted average is also present in the far-field measurements, but is less important as it hardly blurs the larger spots. One can of course still formally define the local time constant as the constant in the exponent, as we have done here, but must keep in mind that it is a weighted average. Near fast recombination centers, the carriers do not diffuse far before they recombine, so the same heuristic ideas used for the far field measurements again apply for the NSOM measurements. This is dramatically illustrated in the high resolution obtained in the images shown here. We are currently considering methods to model this dependence, so that we can be more specific about what the 'local carrier lifetime' measurement yields in a qualitative fashion, for samples of interest to NSOM such as those with regions containing a variety of recombination center types. Here we expect different probe locations to be in different limits of the weighted average issue.

## 6. CONCLUSIONS

We have demonstrated the ability of the NSOM technique to detect inhomogeneities of lifetime of excess carriers in oxygen-terminated silicon wafers. The order of magnitude calculation of free carrier scattering of the IR light is consistent with the experimental results. We have considered the potential effects of tip and sample heating and have found that they are insignificant. Two aspects of the NSOM measurement that differentiate it from its far field counterpart were discussed. First, light in evanescent modes can be coupled into the sample resulting in a higher intensity and k values which are unavailable in the far field. Second, the resolution is high enough that the term local time constant may need to be redefined. Future work will concentrate on refining this technique and seeking new applications.

## 7. ACKNOWLEDGMENTS

We would like to thank Mr Hiroshi Daio, Visiting Scholar in the Materials Science Department at North Carolina State University, for providing the silicon sample used in this experiment and measure the lifetime constant using the laser-microwave technique. This work was supported by the U.S. Army Research Office through grants DAAHO4-94-G-0156 and DAAH04-93-G-0194.

## 8. REFERENCES

1. H.I. Smith and H.G. Craighead, "Nanofabrication", Physics Today, Vol. 43, pp. 24-30, February 1990.

2. D.K. Ferry and R.O. Grondin, Physics of Submicron Devices, Plenum Press, New York, 1991.

3. J. Waldmeyer, "A contactless method for determination of carrier lifetime, surface recombination, velocity, and diffusion constant in semiconductors", J. Appl. Phys., Vol 63, pp. 1977-83,March 1988; D. L. Polla, "Determination of carrier lifetime in Si by optical modulation", IEEE Electron Device Lett. Vol. EDL-4, pp.185-187, June 1983; and G. Bohnert, R. Hacker and A. Hangleiter, "Position resolved carrier lifetime measurements in silicon power devices by time resolved photoluminescence spectroscopy", J. Physique, Vol. C4, pp. 617-620, Sept. 1988.

4. J. W. Goodman, Introduction to Fourier Optics, McGraw Hill, New York, 1968.

5. D. W. Pohl, "Optical stethoscopy: Image recording with resolution λ/20", Appl. Phys Lett, Vol. 44, pp. 651-653, April 1984; and E. Betzig and J. K. Trautman, "Near-field optics: Microscopy, spectroscopy, and surface modification beyond the diffraction limit", Science, Vol. 257, pp. 189-95, July 1992.

6. E. Betzig, P. L. Finn, J. S. Weiner, "Combined shear force and near-field scanning optical microscopy", Appl. Phys. Lett., Vol. 60, pp. 2484,1982; and R. Toledo-Crow, P. C. Yang, Y. Chen, and M. Vaez-Iravani, "Near-field differential scanning optical microscope with atomic force regulation", Appl. Phys. Lett. Vol. 60, pp.2957-59, June 1992.

7. X. Sunney Xie and R. C. Dunn, "probing single molecule dynamics", Science, Vol. 265, pp. 361-364, July 1994; and W. P. Ambrose, P. M. Goodwin, J. C. Martin, R. A. Keller, "Alterations of single molecule fluorescence lifetimes in near-field optical microscopy", Science, Vol. 265, pp. 364-367, July 1994.

8. H. F. Hess, E. Betzig, T. D. Harris, L. N. Pfeiffer, K. W. West, "Near-field spectroscopy of the quantum constituents of a luminescent system", Science, Vol. 264, pp. 1740-45, June 1994.

9 A.H. La Rosa, C.L. Jahncke, and H.D. Hallen, "Time as a Contrast Mechanism in Near-Field Imaging", Ultramicroscopy, in press 1993.

10. P. Moyer, Development, Physics and Applications of Near-Field Scanning Optical microscopy, Ph. D. Thesis, North Carolina State University , 1993.

11. F. J. Sigworth, "Electronic Design of the Patch Clamp", Single-Channel Recording, B.Sakmann and Erwin Neher,ed., pp. 3-35, Plenum Press, New York, 1983.

12. KG-5 glass was obtained from Schott Glass Technologies Inc.

13. F. Shimura, T. Okui, and T. Kusama, "Noncontact minority-carrier lifetime measurement at elevated temperatures for metal-doped Czochralski silicon crystals", J. Appl. Phys., Vol. 67, pp. 7168-71, June 1990.

14. D. K. Schroder, R. N. Thomas, and J. C. Swartz, "Free Carrier Absorption in Silicon," IEEE trans Electron Dev. Vol ED-25, pp. 254-261, Feb. 1978.

15. D. K. Schroder, Semiconductor Material and Device Characterization, John Wiley & Sons, New York, 1990.

16. J. P. Woerdman, "Some Optical and Electrical Properties of a Laser-Generated Free Carrier Plasma in Si," Philips Res. Repts Suppl. No 7, p. 65, 1971.

17. A.H. La Rosa and H. D. Hallen, unpublished.